A study into the impact of sapphire substrate orientation on the properties of nominally-undoped β-Ga₂O₃ thin films grown by pulsed laser deposition

F. H. Teherani, D. J. Rogers, V. E. Sandana, P. Bove, C. Ton-That, et al.

F. H. Teherani, D. J. Rogers, V. E. Sandana, P. Bove, C. Ton-That, L. L. C. Lem, E. Chikoidze, M. Neumann-Spallart, Y. Dumont, T. Huynh, M. R. Phillips, P. Chapon, R. McClintock, M. Razeghi, "A study into the impact of sapphire substrate orientation on the properties of nominally-undoped β-Ga₂O₃ thin films grown by pulsed laser deposition," Proc. SPIE 10105, Oxide-based Materials and Devices VIII, 101051R (23 March 2017); doi: 10.1117/12.2262757

Event: SPIE OPTO, 2017, San Francisco, California, United States

A Study into the Impact of Sapphire Substrate Orientation on the Properties of Nominally-Undoped β-Ga_2O_3 Thin Films Grown by Pulsed Laser Deposition

F. H. Teherani[1], D. J. Rogers[1*], V. E. Sandana[1], P. Bove[1], C. Ton-That[2], L. L. C. Lem[2], E. Chikoidze[3], M. Neumann-Spallart[3], Y. Dumont[3], T. Huynh[2], M. R. Phillips[2], P. Chapon[4], R. McClintock[5] & M. Razeghi[5]

[1]Nanovation, 8 route de Chevreuse, 78117 Châteaufort, France
[2]School of Mathematical & Physical Science, University of Technology Sydney, Australia
[3]Groupe d'Etudes de la Matière Condensée, UVSQ-CNRS, Paris Saclay University, Versailles, France
[4]P. Chapon, Horiba France, 16-18 rue du Canal, Longjumeau, 91165, France
[5]Center for Quantum Devices, Northwestern University, Evanston, Illinois, USA

Corresponding author email: rogers@nanovation.com

ABSTRACT

Nominally-undoped Ga_2O_3 layers were deposited on *a-, c-* and *r*-plane sapphire substrates using pulsed laser deposition. Conventional x-ray diffraction analysis for films grown on *a-* and *c*-plane sapphire showed the layers to be in the β-Ga_2O_3 phase with preferential orientation of the (-201) axis along the growth direction. Pole figures revealed the film grown on *r*-plane sapphire to also be in the β-Ga_2O_3 phase but with epitaxial offsets of 29.5°, 38.5° and 64° from the growth direction for the (-201) axis. Optical transmission spectroscopy indicated that the bandgap was ~5.2eV, for all the layers and that the transparency was > 80% in the visible wavelength range. Four point collinear resistivity and Van der Pauw based Hall measurements revealed the β-Ga_2O_3 layer on r-plane sapphire to be 4 orders of magnitude more conducting than layers grown on *a-* and *c*-plane sapphire under similar conditions. The absolute values of conductivity, carrier mobility and carrier concentration for the β-Ga_2O_3 layer on *r*-sapphire (at 20 $\Omega^{-1}.cm^{-1}$, 6 cm^2/Vs and 1.7 x 10^{19} cm^{-3}, respectively) all exceeded values found in the literature for nominally-undoped β-Ga_2O_3 thin films by at least an order of magnitude. Glow discharge optical emission spectroscopy compositional depth profiling for common shallow donor impurities (Cl, Si and Sn) did not indicate any discernable increase in their concentrations compared to background levels in the sapphire substrate. It is proposed that the fundamentally anisotropic conductivity in β-Ga_2O_3 combined with the epitaxial offset of the (-201) axis observed for the layer grown on *r*-plane sapphire may explain the much larger carrier concentration, electrical conductivity and mobility compared with layers having the (-201) axis aligned along the growth direction.

1. INTRODUCTION

Recently there have been many publications focused on monoclinic β-Ga_2O_3 in bulk crystal, thin film and nanostructured forms [1]. β-Ga_2O_3 is the most common, stable and studied phase amongst a large family of reported Ga_2O_3 polymorphs and it exhibits a distinctive and tunable property including a direct wide bandgap (E_g ~ 4.85 eV), an orientation-dependent thermal conductivity and an n-type conductivity that can be stoichiometrically tuned (for bulk crystals) from 10^{-9} $\Omega^{-1}.cm^{-1}$ (when stoichiometric and predominantly impurity-free) to highly conductive 38 $\Omega^{-1}.cm^{-1}$ [2] (when oxygen deficient). β-Ga_2O_3 also has a relatively high breakdown voltage compared with other wide bandgap materials, such as GaN or

Oxide-based Materials and Devices VIII, edited by Ferechteh H. Teherani, David C. Look,
David J. Rogers, Ivan Bozovic. Proc. of SPIE Vol. 10105, 101051R · © 2017 SPIE
CCC code: 0277-786X/17/$18 · doi: 10.1117/12.2262757

SiC. Furthermore, by alloying with Mg [3] bandgap engineering further into the UV has also been demonstrated. These properties/potentialities, along with the recent appearance of commercial single crystal bulk substrates, have generated considerable interest of late for the adoption of β-Ga_2O_3 in a number of important technological applications from transparent electrodes, thin film transistors and gas sensors to UVC photodetectors and LEDs [5-7]. However, several features of β-Ga_2O_3 remain contentious in the literature, including the nature of the shallow donors in nominally-undoped but oxygen-poor β-Ga_2O_3. Indeed, *n*-type conductivity was commonly attributed in the past to the presence of ionized oxygen vacancies. However, this notion has been thrown into question of late [8] by DFT calculations which suggest that oxygen vacancies are deep donors (with an ionization energy of more than 1 eV) and thus cannot contribute to *n*-type conductivity. Subsequently, it was proposed that hydrogen and or background impurities (such as Si, Ge, F, Cl or Sn) may be implicated in the *n*-type conduction invariably observed in nominally-undoped β-Ga_2O_3. This study involves the investigation of the electrical and optical properties in nominally-undoped β-Ga_2O_3 thin films grown by Pulsed Laser Deposition (PLD) in order to further explore this topic.

2. EXPERIMENT

Ga_2O_3 layers were grown on *a*-, *c*- and *r*-plane sapphire substrates by PLD from a commercial sintered 4N Ga_2O_3 target using a Coherent LPX KrF (λ = 248nm) laser. Uniform 2 inch diameter wafer coverage was obtained using optical rastering of the incident laser beam. Substrate temperature during growth was measured with a thermocouple to be ~550°C and the ambient during growth was 10^{-4} torr of molecular oxygen. Room temperature (RT) optical transmission studies were performed using an Ocean Optics system comprising a halogen lamp, a deuterium lamp and a Maya optical spectrometer. Film thickness was estimated using optical reflection interferometry with an Ocean Optics Nanocalc system. Sample morphology was examined using a Philips S800 field emission gun-Scanning Electron Microscope (FEG-SEM). The crystal structure of the samples was investigated using high resolution X-Ray Diffraction (XRD) performed in a Panalytical MRD Pro system using Cu $K\alpha_1$ radiation. Electrical resistivity was measured with a Signatone four-collinear-probe system equipped with a Keithley 2400 source-meter. Hall measurements were made at room temperature in Van der Pauw configuration using an Ecopia HMS3000 system with a 1T magnet and indium-soldered Ohmic contacts. Cathodoluminescence (CL) was performed using a FEI Quanta 200 SEM equipped with a parabolic mirror light collector and an Ocean Optics QE65000 spectrometer. Pulsed radio frequency Glow Discharge Optical Emission Spectroscopy (GDOES) compositional depth profiling was performed using a Jobin-Yvon GD profiler 2 system.

3. RESULTS

3.1 Structural & Morphological Characterisation

Figure 1 shows the XRD 2θ/ω scans for the Ga_2O_3 on the three different sapphire substrate orientations. For the growths on the *c*-and *a*-sapphire, the peaks were typical for β-Ga_2O_3 with a preferential (-201) alignment along the growth direction. For the *r*-plane substrate, however, there are only weak peaks. Nakagomi et al. [9] identified similar peaks as potentially being from β-Ga_2O_3 (201) and (402) reflections.

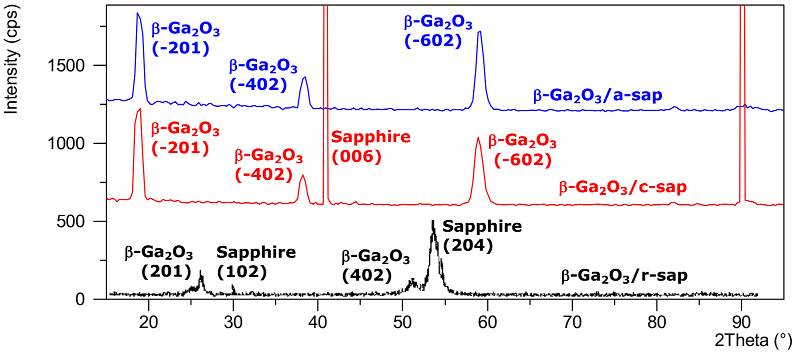

Figure 1. XRD $2\theta/\omega$ scans for Ga_2O_3 layers grown on three different sapphire substrate orientations.

Figure 2 shows an XRD pole figure for the (-402) peak of β-Ga_2O_3 for the growth on *r*-plane sapphire.

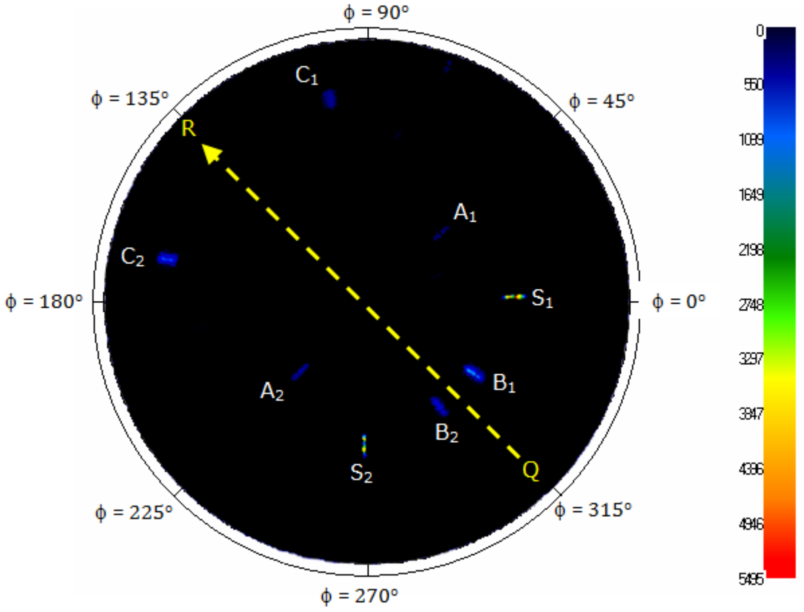

Figure 2 XRD pole figure (χ: 0 ➔ 85° and ϕ: 0➔ 360°) for the β-Ga_2O_3 (-402) plane in the layer grown on an *r*-plane sapphire substrate.

The figure shows four distinct pairs of diffraction points with rotational symmetry about the QR axis. From their much narrower and more intense peaks, spots S_1 and S_2 ($\chi \sim 43.25°$) can be identified as originating from the substrate. In their XRD pole figures for (thermally-evaporated) β-Ga_2O_3 layers on *r*-plane sapphire, Nakagomi et al. [9] identified comparable spots to S_1 and S_2 ($\chi \sim 43.25°$) as originating from the (110) plane sapphire of the *r*-sapphire substrate. They also identified comparable spots to A_1 and A_2 ($\chi \sim 29.5°$) as originating from β-Ga_2O_3 (-201) planes growing almost parallel to the *r*-sapphire (113) and/or (2-13) axes (which are both rotated by 27° from the (102) surface of the *r*-plane sapphire). The χ value for the spots B_1 and B_2 (38.5°) is quite similar to the substrate S_1 and S_2 spots, suggesting (-201) planes growing with an offset of about 4.75° from the *r*-sapphire (110) planes, while the spots C_1 and C_2 show a χ of about 64°. Interestingly, Nakagomi et al. [9] did not observe the B and C pairs of spots.
Figure 3 shows SEM images for the β-Ga_2O_3 layers grown on the three different sapphire orientations.

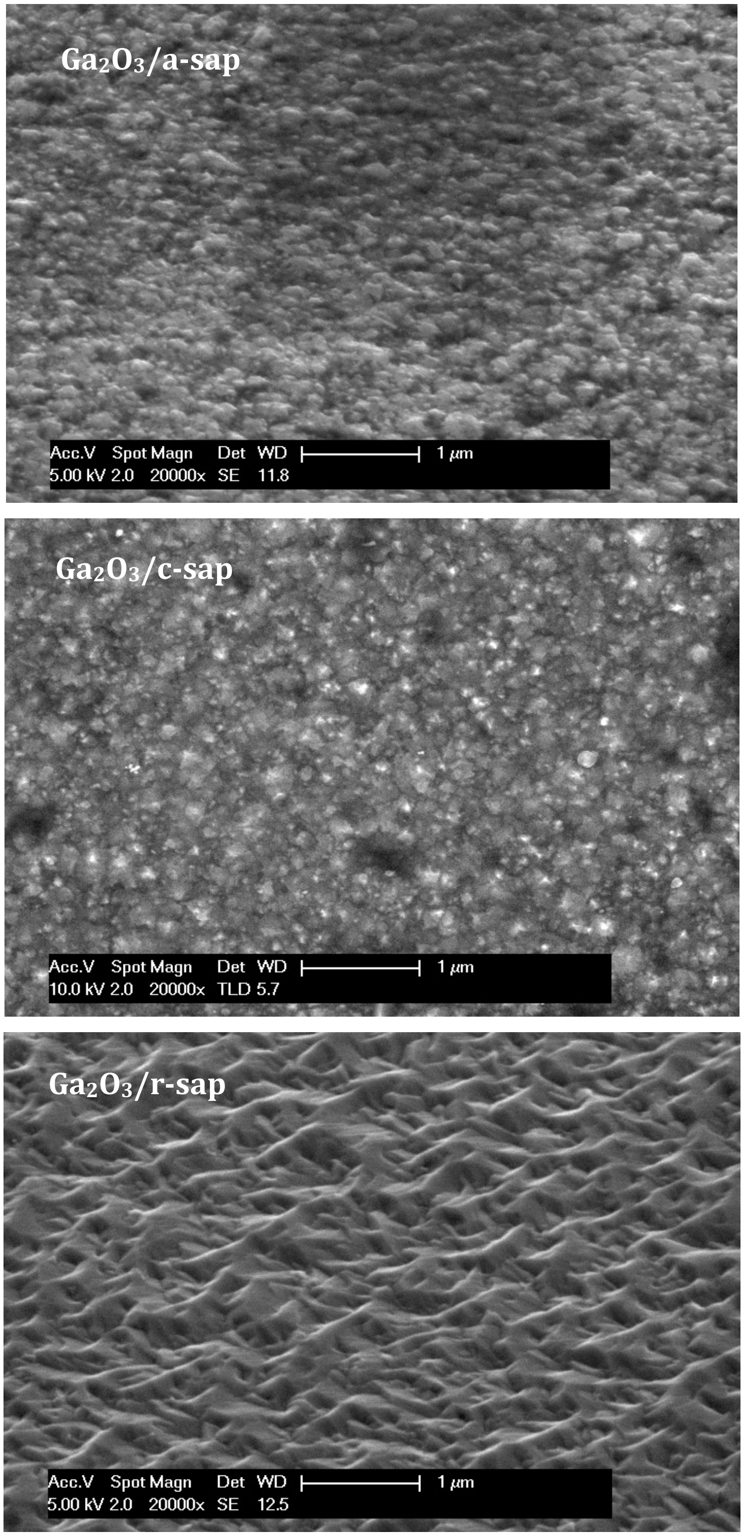

Figure 3. SEM images for the β-Ga_2O_3 layers grown on the three different sapphire substrate orientations.

The layers on *a*- and *c*-plane sapphire both exhibit a fine granular surface morphology resembling an irregular agglomeration of particulates (on a tens-of-nm scale) while the layer on *r*-plane sapphire exhibits a coarser morphology with non-granular peaks having smooth side walls (resembling crystal facets). Furthermore, connecting ridges between many of these peaks show a distinct preferential diagonal orientation (running from bottom-left to top-right in the above image). This is coherent with the β-Ga_2O_3 layer grown on *r*-sapphire having an epitaxial relationship with the substrate.

3.2 Optical Characterization

Figure 4 shows optical transmission spectra for the Ga_2O_3 layers grown on the three different sapphire substrate orientations.

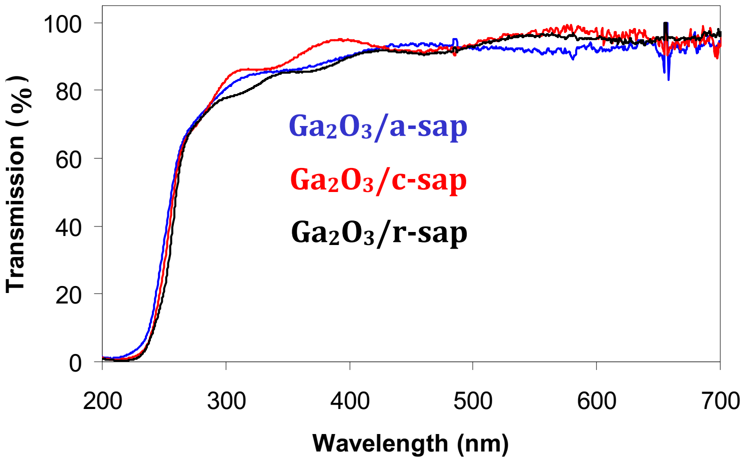

Figure 4 Optical transmission spectra for β-Ga_2O_3 layers grown on three different sapphire orientations.

The optical transmission spectra all show transparency of over 80% for wavelengths above the UVC range and the absorption edges all indicate bandgaps of about 5.2 eV. The value is slightly higher than would be expected for β-Ga_2O_3, which is probably due to bandgap renormalisation.

Figure 5 shows 300K CL spectra for the β-Ga_2O_3 layers grown on the three different sapphire orientations.

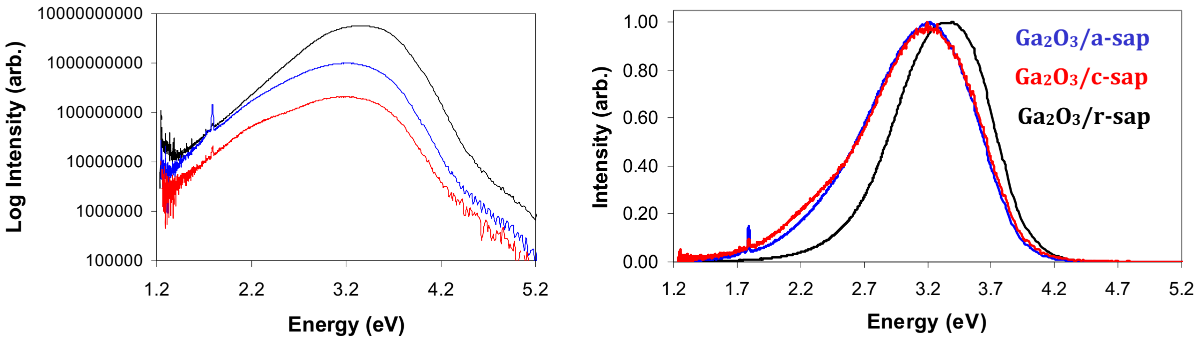

Figure 5. Log scale and normalised 300K CL spectra for the β-Ga_2O_3 layers grown on the three different sapphire substrate orientations.

The CL spectra revealed a relatively wide UV band peaked at 3.37 eV for the growth on *r*-plane sapphire which broadened and red-shifted to 3.20 eV for the layers grown on *a*- and *c*-plane sapphire. Under identical CL excitation conditions (E_B = 4 keV, I_B = 15 nA), the layer on *r*-sapphire exhibits stronger emission, roughly by an order of magnitude, than the layers grown on *a*- or *c*-sapphire, indicating greater crystalline quality for the layer with epitaxial offset of the β-Ga_2O_3 (-201) orientation. The linewidth was also significantly narrower (at 0.88 eV) for the *r*-plane sapphire than for the other two sapphire orientations (at 1.02 ± 0.01 eV).

3.3 Electrical Transport Properties

Table 1 shows the results of the collinear four point resistance and RT Hall measurements

Substrate	**Ga_2O_3 Thickness (optical interferometry)**	**Collinear four-point resistivity**	**Hall-effect measurement**		
	(nm)	**$\rho(\Omega.cm)$**	**VdP ρ (Ω.cm)**	**n (cm^{-3})**	**μ (cm^2/Vs)**
***a*-sapphire**	180	320	-	-	-
***c*-sapphire**	335	∞	-	-	-
***r*-sapphire**	365	0.03	0.05	1.7×10^{19}	6

Table: 1 Film thicknesses, collinear four-point resistivities and Hall measurement data for β-Ga_2O_3 layers grown on *a*-, *c*- and *r*-plane sapphire substrates.

While the resistivity of the β-Ga_2O_3 grown on *a*- plane sapphire was 320 Ω.cm and that on *c*-plane sapphire was above the measurement capacity of the Keithley 2400 Source-Meter, the β-Ga_2O_3 grown on *r*-plane sapphire showed a value of 3×10^{-2} Ω.cm, which is exceptionally low in absolute terms for undoped β-Ga_2O_3. Hall-effect measurements were not possible (with the Ecopia HMS 3000 system) for the highly resistive layers on *c*- and *a*- plane sapphire. For the layer on *r*-sapphire, Hall measurements confirmed the low resistivity and indicated n-type conduction with a carrier concentration of 1.7×10^{19} cm^{-3} and a mobility of 6 cm^2/Vs. These values are also very high in absolute terms for undoped β-Ga_2O_3.

3.4 Compositional Analysis

Since the conductivity and mobility found for the β-Ga_2O_3 layer grown on *r*-sapphire are significantly higher than values reported for thin films elsewhere in the literature (for both nominally-undoped or intentionally doped material [10]) it was decided to investigate the level of unintentional impurities in the layers. Figure 7 displays GDOES depth profiles for the β-Ga_2O_3 grown on r-plane sapphire. The upper plot shows the concentration profiles of gallium and aluminium as a function of etch time. The region where the Ga concentration drops indicates the etch depth of the substrate/layer interface. Based on this positioning of the interface depth, it can be deduced that the Al concentration has a tail extending into the β-Ga_2O_3 layer. This could be due to the significant surface roughness causing ambiguity in the interface position or it could be due to diffusion of the Al from the substrate into the β-Ga_2O_3 layer. Such Al doping would not be expected to increase the carrier concentration, however, because Al (with a 3+ valence) is unlikely to be a donor in β-Ga_2O_3 and alloying of β-Ga_2O_3 with Al is actually an established method to increase the bandgap energy.

The lower plot of the GDOES compositional depth profile for the potential shallow donors in Ga_2O_3 shows that the concentrations of the common shallow acceptors Cl, Si and Sn [1] were relatively low compared to the Al and Ga levels and that they did not present any significant enhancement in the β-Ga_2O_3 layer compared to their background levels in the *r*-Al_2O_3 substrate.

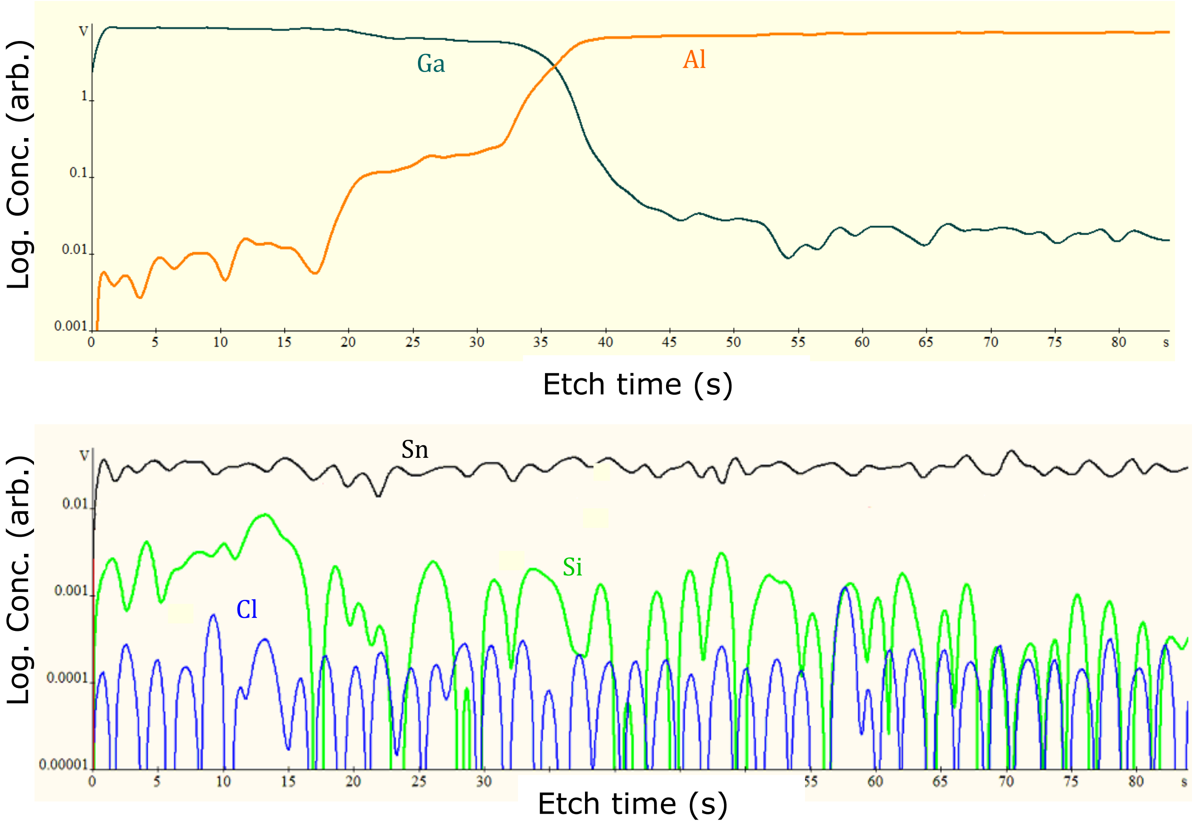

Figure 7 Uncalibrated GDOES compositional depth profiles (log scale) for selected elements in the β-Ga_2O_3 grown on *r*-plane sapphire. The upper and lower plots were from the same acquisition but different y scales are used so as to reveal the profile forms for elements with significantly different concentration levels.

4. DISCUSSION

Based on the GDOES studies and the fact that all the layers were deposited using the same target, the 4 order of magnitude increase in conductivity does not seem to be due to unintentional impurity doping. Relatively large variations of resistivity (between 1 and 200 Ω.cm) have also been reported by other groups for nominally-undoped β-Ga_2O_3 thin films grown on silicon substrates. These variations were explained to be the result of a difference in crystalline quality due to different growth temperatures [11] but this mechanism does not seem to be relevant as an explanation for the resistivity variations we observe because all the layers were grown in the same temperature range.

Resistivities as low as 1.5×10^{-1} Ω.cm have been reported for nominally-undoped β-Ga_2O_3 thin layers grown on c-sapphire substrates by PLD [12] and were explained to be a result of a relatively high deposition temperature (1000°C) producing large grain sizes (i.e. reduced scattering probability for charge carriers). Our growth temperature was significantly lower, however.

Finally, strong anisotropy of conductivity along the directions of b and c axes has been reported for bulk crystals of β-Ga_2O_3 [13] and explained to be the result of a difference in the electron wave-function overlap between adjacent donors. Since the layer on r-sapphire showed an epitaxial offset of the (-201) axis, this could be a possible explanation for the extraordinary electrical properties.

5. CONCLUSIONS

Nominally-undoped Ga_2O_3 layers were deposited on *a*-, *c*- and *r*-plane sapphire substrates by PLD. XRD showed all the layers to be in the β-Ga_2O_3 phase and while the films grown on *a*- and *c*-plane sapphire had strong preferential orientation of the (-201) axis along the growth direction, the layer grown on *r*-plane sapphire showed epitaxial growth with the (-201) axis tilted at χ of 29.5° 38.5° and 64° from the normal to the substrate (102) surface plane. SEM revealed a peaked surface morphology with smooth (facet-like) side-walls and preferentially-oriented connecting ridges for the layer grown on *r*-sapphire, whereas the layers grown on *a*- and *c*-plane sapphire both showed a more irregular surface morphology with a finer granular appearance. Optical transmission spectroscopy suggested that the bandgap was about ~5.2eV, for all the layers and transparency was > 80% for wavelengths over the UVC range. The β-Ga_2O_3 layer on *r*-plane sapphire also showed much stronger CL intensity, narrower linewidths and a slight blueshift. These indicate that the crystal quality was higher for these layers than for those grown on *a*- and *c*-plane sapphire. Four point collinear resistivity and Van der Pauw based Hall measurements revealed the β-Ga_2O_3 layer on r-plane sapphire to be at least 4 orders of magnitude more conducting than layers grown on *a*- and *c*-plane sapphire under similar conditions. The absolute values of conductivity, carrier mobility and carrier concentration all exceeded values found in the literature for nominally-undoped β-Ga_2O_3 by at least an order of magnitude. GDOES compositional depth profiling for common shallow donor impurities (Cl, Si and Sn) did not reveal any significant increase compared to their background levels in the sapphire substrate, however. It is suggested that the fundamentally anisotropic conductivity in β-Ga_2O_3 combined with the epitaxial offset of the (-201) axis observed for the layer grown on *r*-plane sapphire may explain the much larger carrier concentration, electrical conductivity and mobility compared with layers having the (-201) axis aligned along the growth direction.

REFERENCES

1. S. I. Stepanov, V. I. Nikolaev, V. E. Bougrov and A. E. Romanov Rev. Adv. Mater. Sci. 44 (2016) 63 – 86
2. N. Ueda, H. Hosono, R. Waseda and H. Kawazoe Appl. Phys. Lett. 70 (1997) 3561.
3. X. Feng, Z. Li, W. Mi, Y. Luo and J. Ma Mater. Sci. Semicond. Process 34 (2015) 52
4. N. Suzuki, S. Ohira, M. Tanaka, T. Sugawara, K. Nakajima & T. Shishido: Phys. Status Solidi C 4 (2007) 2310.
5. K. Matsuzaki, H. Yanagi, T. Kamiya, H. Hiramatsu, K. Nomura, M. K. Matsuzaki, H. Yanagi, T. Kamiya, H. Hiramatsu, K. Nomura, M. Hirano, and H. Hosono: Appl. Phys. Lett. 88 (2006) 092106
6. T. Oshima, T. Okuno, and S. Fujita: Jpn. J. Appl. Phys. 46 (2007) 7217.
7. R. Roy, V. G. Hill, and E. F. Osborn: J. Am. Chem. Soc. 74 (1952) 719.
8. J. B. Varley, J. R. Weber, A. Janotti and C. G. Van de Walle, Appl. Phys. Lett. 97 (2010) 142106
9. S. Nakagomi, S. Kaneko, and Y. Kokubun Phys. Status Solidi B 252, No. 3, 612–620 (2015)
10. T. Onuma, S. Fujioka, T. Yamaguchi, M. Higashiwaki, K. Sasaki, T. Masui, and T. Honda: Appl. Phys. Lett. 103 (2013), 041910
11. C.V.Ramana, E.J.Rubio, C.D.Barraza, A.M. Gallardo, S.McPeack, S.Kortu, J.T.Grant, J. Appl. Phys. 115, 043508 (2014)
12. S-L. Ou, D_S. Wuu, Y-C.Fu, Sh-P.Liu, R. H. Horng, L.Liu, Zh-Ch.Feng, J. Mat. Chem. & Phys. 133, 700, (2012))
13. N. Ueda, H. Hosono, R. Waseda and H. Kawazoe Appl. Phys. Lett. **71,** 7, (1997)